

Anisotropic quantum scattering in plane

Eugene A. Koval,^{1,2,*} Oksana A. Koval,^{1,†} and Vladimir S. Melezhik^{1,2,‡}

¹*Bogoliubov Laboratory of Theoretical Physics, Joint Institute for Nuclear Research,
Dubna, Moscow Region 141980, Russian Federation*

²*Department of Theoretical Physics, Dubna International University for Nature,
Society and Man, Dubna, Moscow Region 141980, Russian Federation*

(Dated: March 19, 2014)

We study the quantum scattering in two spatial dimensions (2D). Our computational scheme allows to quantitatively analyze the scattering parameters for the strong anisotropy of the interaction potential. High efficiency of the method is demonstrated for the 2D scattering on the cylindrical potential with the elliptical base and dipole-dipole collisions in the plane. We reproduce the result for the 2D scattering of polarized dipoles in binary collisions obtained recently by Ticknor [Phys. Rev. A **84**, 032702 (2011)] and explore the 2D collisions of unpolarized dipoles.

PACS numbers: 31.15.ac, 31.15.xf, 34.50.Cx, 34.50.-s

I. INTRODUCTION

In recent years, the problem of anisotropic quantum scattering in two spatial dimensions (2D) attracts increasing interest. It is stimulated by spectacular proposals for prospects to create exotic and highly correlated quantum systems with dipolar gases [1, 2]. Particularly, there were considered anisotropic superfluidity [3], 2D dipolar fermions [4], and few-body dipolar complexes [5]. The recent experimental production of ultracold polar molecules in confined geometry of optical traps [6–8] has opened up ways to realize these phenomena. Noteworthy also is rather long history of research of 2D quantum effects in condensed matter physics. One can note superfluid films [9], high-temperature superconductivity [10], 2D materials, such as graphene [11], and even possibilities for topological quantum computation [12]. Unique opportunities for modeling these 2D effects in a highly controlled environment have appeared recently with the development of experimental techniques for creation of quasi-2D Bose and Fermi ultracold gases [13].

Interest in the processes and effects in 2D-geometry has stimulated the theory of elementary quantum two-body systems and processes in the plane. Special consideration should be given to the anisotropy and long-range character of the dipole-dipole interaction. Actually, usual partial-wave analysis becomes inefficient for describing the dipole-dipole scattering due to the strong anisotropic coupling of different partial-waves in the asymptotic region [14, 15]. Recently, considerable progress in the analysis of the 2D and quasi-2D (q2D) scattering of dipoles has been achieved [16–20]. Thus, the 2D dipolar scattering in the threshold and semiclassical regimes was studied in the case of the dipole polarization directed orthogonally to the scattering plane [16]. Arbitrary angle of

polarization was considered in [17].

In this work, we develop a method for quantitative analysis of the 2D quantum scattering on a long-range strongly anisotropic scatterer. Particularly, it permits the description of the 2D collisions of unpolarized dipoles. Our approach is based on the method suggested in [21] for the few-dimensional scattering which was successfully applied to the dipole-dipole scattering induced by an elliptically polarized laser field in the 3D free-space [15].

The key elements of the method are described in Section II. In Section III, we apply the method to the 2D scattering on the cylindrical potential with the elliptical base and the 2D dipole-dipole scattering of unpolarized dipoles. We reproduce the threshold formula [22, 23] for the scattering amplitude on the cylinder potential with the circular base and the results of [16, 17] for the 2D scattering of polarized dipoles. High efficiency of the method has been found in all problems being considered. The last Section contains the concluding remarks. Some important details of the computational scheme and illustration of the convergence are given in Appendices.

II. 2D SCATTERING PROBLEM IN ANGULAR GRID REPRESENTATION

The quantum scattering on the anisotropic potential $U(\rho, \phi)$ in the plane is described by the 2D Schrödinger equation in polar coordinates (ρ, ϕ)

$$H(\rho, \phi)\Psi(\rho, \phi) = E\Psi(\rho, \phi) \quad (1)$$

with the scattering boundary conditions

$$\Psi(\rho, \phi) \rightarrow e^{i\mathbf{q}\rho} + f(\mathbf{q}, \phi, \phi_q) \frac{e^{i\mathbf{q}\rho}}{\sqrt{-i\rho}} \quad (2)$$

in the asymptotic region $\rho \rightarrow \infty$ and the Hamiltonian of the system

$$H(\rho, \phi) = -\frac{\hbar^2}{2\mu} \left(\frac{1}{\rho} \frac{\partial}{\partial \rho} \left(\rho \frac{\partial}{\partial \rho} \right) + \frac{1}{\rho^2} h^{(0)}(\phi) \right) + U(\rho, \phi).$$

* e-cov@yandex.ru

† kov.oksana20@gmail.com

‡ melezhik@theor.jinr.ru

The unknown wave function $\Psi(\rho, \phi)$ and the scattering amplitude $f(q, \phi, \phi_q)$ are searched for the fixed momentum \mathbf{q} defined by the colliding energy E ($q = \sqrt{2\mu E}/\hbar$) and the direction \mathbf{q}/q of the incident wave (defined by the angle ϕ_q) and for the scattering angle ϕ ¹. Here μ is the reduced mass of the system. In the polar coordinates, the angular part of the kinetic energy operator in $H(\rho, \phi)$ has a simple form $h^{(0)}(\phi) = \frac{\partial^2}{\partial \phi^2}$. The interaction potential $U(\rho, \phi)$ can be anisotropic in the general case, i.e. to be strongly dependent on ϕ . It is clear that varying the direction of the incident wave \mathbf{q}/q can be replaced by the rotation $U(\rho, \phi) \rightarrow U(\rho, \phi + \phi_q)$ of the interaction potential by the angle ϕ_q for the fixed direction of the incident wave, which we choose to be coincident with the x-axis. Thus, in the case of anisotropic potential $U(\rho, \phi)$ the task is to solve the problem (1) with the interaction potential $U(\rho, \phi + \phi_q)$ for all possible ϕ_q and fixed E with the scattering boundary conditions

$$\Psi(\rho, \phi) \rightarrow \exp\{iq\rho \cos(\phi)\} + f(q, \phi, \phi_q) \frac{e^{iq\rho}}{\sqrt{-i\rho}}. \quad (3)$$

If the scattering amplitude $f(q, \phi, \phi_q)$ is found, one can calculate the differential scattering cross section

$$d\sigma(q, \phi, \phi_q)/d\Omega = |f(q, \phi, \phi_q)|^2, \quad (4)$$

where $d\Omega = d\phi d\phi_q$, as well as the total cross section

$$\sigma(q) = \frac{1}{2\pi} \int_0^{2\pi} \int_0^{2\pi} \frac{d\sigma}{d\Omega} d\phi_q d\phi \quad (5)$$

by averaging over all possible orientations ϕ_q of the scatterer and integration over the scattering angle ϕ .

To integrate the problem (1),(2), we use the method suggested in [21] to solving a few-dimensional scattering problem and applied in [15] for the dipole-dipole scattering in the 3D free-space. Following the ideas of these works we choose the eigenfunctions

$$\xi_m(\phi) = \frac{1}{\sqrt{2\pi}} e^{im(\phi-\pi)} = \frac{(-1)^m}{\sqrt{2\pi}} e^{im\phi} \quad (6)$$

of the operator $h^{(0)}(\phi)$ as a Fourier basis for the angular grid representation of the searched wave-function $\Psi(\rho, \phi)$. We introduce the uniform grid $\phi_j = \frac{2\pi j}{2M+1}$ (where $j = 0, 1, \dots, 2M$) over the ϕ and ϕ_q -variables and search the wave function as expansion

$$\begin{aligned} \Psi(\rho, \phi) &= \frac{1}{\sqrt{\rho}} \sum_{j=0}^{2M} \sum_{m=-M}^M \xi_m(\phi) \xi_{mj}^{-1} \psi_j(\rho) = \\ &= \frac{2\pi}{\sqrt{\rho}} \left(\frac{1}{2M+1} \right) \sum_{j=0}^{2M} \sum_{m=-M}^M e^{im(\phi-\phi_j)} \psi_j(\rho), \end{aligned} \quad (7)$$

where $\xi_{mj}^{-1} = \frac{2\pi}{2M+1} \xi_{jm}^* = \frac{2\pi}{2M+1} e^{-im\phi_j}$ is the inverse matrix to the $(2M+1) \times (2M+1)$ square matrix $\xi_{jm} = \xi_m(\phi_j)$ defined on the angular grid².

In the representation (7) the unknown coefficients $\psi_j(\rho)$ are defined by the values of the searched wave function on the angular grid $\psi_j(\rho) = \sqrt{\rho} \Psi(\rho, \phi_j)$, any local interaction is diagonal

$$\begin{aligned} U(\rho, \phi) \Psi(\rho, \phi) |_{\phi=\phi_j} &= \\ &= \frac{2\pi}{(2M+1)\sqrt{\rho}} U(\rho, \phi_j) \sum_{j'=0}^{2M} \sum_{m=-M}^M e^{im(\phi_j-\phi_{j'})} \psi_{j'}(\rho) \quad (8) \\ &= \frac{1}{\sqrt{\rho}} U(\rho, \phi_j) \psi_j(\rho), \end{aligned}$$

and the angular part $h_{jj'}^{(0)}$ of the kinetic energy operator has a simple form

$$\begin{aligned} h^{(0)}(\phi) \Psi(\rho, \phi) |_{\phi=\phi_j} &= \frac{1}{\sqrt{\rho}} \sum_{j'=0}^{2M} h_{jj'}^{(0)} \psi_{j'}(\rho) \\ &= -\frac{2\pi}{(2M+1)\sqrt{\rho}} \sum_{j'=0}^{2M} \left(\sum_{m=-M}^M m^2 e^{im(\phi_j-\phi_{j'})} \right) \psi_{j'}(\rho). \end{aligned} \quad (9)$$

Note that the presence in the interaction potential of the “nonlocal” angular part (i.e. the integration or differentiation over angular variable) leads to destroying the diagonal structure in (8).

Thus, the 2D Schrödinger equation (1) is reduced in the angular grid representation (7) to the system of $2M+1$ coupled ordinary differential equations of the second order:

$$\begin{aligned} \frac{d^2 \psi_j(\rho)}{d\rho^2} + \frac{2\mu}{\hbar^2} \left(E - U(\rho, \phi_j) + \frac{\hbar^2}{8\mu\rho^2} \right) \psi_j(\rho) + \\ + \frac{1}{\rho^2} \sum_{j'} h_{jj'}^{(0)} \psi_{j'}(\rho) = 0. \end{aligned} \quad (10)$$

Since the wave function $\Psi(\rho, \phi_j) = \frac{\psi_j(\rho)}{\sqrt{\rho}}$ must be finite at the origin $\left(\frac{\psi_j(\rho)}{\sqrt{\rho}} \rightarrow \text{const} \right)$, the “left-side” boundary condition for the functions $\psi_j(\rho)$ reads as

$$\psi_j(\rho \rightarrow 0) \rightarrow \text{const} \sqrt{\rho} \quad (j = 0, 1, \dots, 2M). \quad (11)$$

In the asymptotic region $\rho \rightarrow \infty$ the scattering boundary condition (3) accepts the form

$$\begin{aligned} \frac{2\pi}{\sqrt{\rho}(2M+1)} \sum_{j=0}^{2M} \sum_{m=-M}^M e^{im(\phi-\phi_j)} \psi_j(\rho) = \\ = \exp\{iq\rho \cos(\phi)\} + f(q, \phi, \phi_q) \frac{e^{iq\rho}}{\sqrt{-i\rho}}. \end{aligned} \quad (12)$$

² To calculate the inverse matrix ξ_{mj}^{-1} , we use the completeness relation for the Fourier basis $\sum_{m=-\infty}^{\infty} \xi_m(\phi_k) \xi_m^*(\phi_j) = \delta(\phi_k - \phi_j)$, which in our grid representation reads $\sum_{m=-M}^M \xi_{km} \xi_{jm}^* = \frac{2M+1}{2\pi} \delta_{kj}$.

¹ Hereafter we use the definition of the scattering amplitude introduced in [24].

By using the Fourier expansion for the plane wave $\exp\{iq\rho\cos(\phi)\}$ and the scattering amplitude $f(q, \phi, \phi_q)$ ³

$$\exp\{iq\rho\cos(\phi)\} = \sum_{m'=-M}^M i^{m'} J_{m'}(q, \rho) e^{im'\phi} \quad (13)$$

$$f(q, \phi, \phi_q) = \frac{1}{\sqrt{2\pi}} \sum_{m'=-M}^M f_{m'}(\phi_q) e^{im'\phi} \quad (14)$$

we eliminate the angular dependence from the asymptotic equation (12) and represent the “right-side” boundary condition for the functions $\psi_j(\rho \rightarrow \infty)$ in the form

$$\frac{2\pi}{(2M+1)\sqrt{\rho}} \sum_{j=0}^{2M} e^{-im\phi_j} \psi_j(\rho) = i^m J_m(q\rho) \sqrt{2\pi} + \frac{f_m(\phi_q)}{\sqrt{-i\rho}} e^{iq\rho}. \quad (15)$$

To solve the boundary-value problem (10), (11) and (15), we introduce the grid over the ρ -variable $\{\rho_n\}$ ($n = 0, 1, \dots, N$) and reduce the system of differential equations (10) by using the finite-difference approximation of the sixth order to the system of $(N+1) \times (2M+1)$ algebraic equations

$$\hat{A}\psi = 0 \quad (16)$$

with the band-structure of the matrix \hat{A} with the width $(2M+1) \times 7$ of the band. By using the asymptotic equations (15) in the last two points ρ_{N-1} and ρ_N one can eliminate the unknown vector $f_m(\phi_q)$ from equation (15) and rewrite the “right-side” boundary condition in the form

$$\sum_{j'} \{A_{jj', NN-1} \psi_{j'}(\rho_{N-1}) + A_{jj', NN} \psi_{j'}(\rho_N)\} = F_{j,N}(q, \rho_{N-1}, \rho_N). \quad (17)$$

Analogously, one can eliminate unknown constant from expression (11) by considering asymptotic equations (11) at the first points ρ_0, ρ_1 and ρ_1 . The acquired “left-side” boundary condition reads

$$\psi_j(\rho_0 = 0) = 0, \quad \sum_{j'} \{A_{jj', 11} \psi_{j'}(\rho_1) + A_{jj', 12} \psi_{j'}(\rho_2)\} = F_{j,1}(q, \rho_1, \rho_2). \quad (18)$$

³ Here $J_m(q, \rho)$ are the first kind Bessel functions of integer order. Their asymptotic behavior [25]:

$$J_m(z) \xrightarrow{|z| \rightarrow \infty} \sqrt{\frac{2}{\pi z}} \cos\left(z - \frac{m\pi}{2} - \frac{\pi}{4}\right) + e^{|Imz|} O(|z|^{-1}), \quad (|\arg(z)| < \pi)$$

Thus, the scattering problem is reduced to the boundary value problem (16-18)

$$\hat{A}\psi = F, \quad (19)$$

which can be efficiently solved with standard computational techniques such as the sweeping method [26] or the LU-decomposition [27]. The detailed structure of the matrix of the coefficients $A_{jj', nn'}$ is discussed in Appendix A. After the solving of Eq.(19) and finding the wave function $\psi_j(\rho)$ the scattering amplitude $f(q, \phi, \phi_q)$ is constructed according to Eqs.(15) and (14).

III. RESULTS AND DISCUSSIONS

A. Scattering on anisotropic scatterer

First, we have analyzed the 2D scattering on the cylindrical potential barrier with the elliptical base

$$U(\rho, \phi) = \begin{cases} U_0, & \rho \leq a(\phi) \\ 0, & \rho > a(\phi) \end{cases} \quad (20)$$

The case of the circular base $a(\phi) = a_0$ was considered in [22, 23], where analytic formula for the scattering amplitude

$$f(q) \rightarrow -\sqrt{\frac{\pi}{2q}} \frac{1}{\ln \left[\frac{2}{\gamma q a_{2D}} \right] + i \frac{\pi}{2}} \quad (21)$$

was obtained in the zero-energy limit $q \rightarrow 0$. Here $\gamma = \exp(C)$ and $C = 0.577\dots$ is the Euler constant. We have analyzed the scattering on the potential barrier with circular base $a(\phi) = a_0$ for arbitrary momentum q . The results of calculation presented in Figs. 1 and 2 confirm the convergence of the scattering amplitude $f(q, \phi, \phi_q)$ to the analytical value (21) at $q \rightarrow 0$. Hereafter all the calculations were performed in the units $\hbar = \mu = 1$.

In the limiting case of the infinitely high potential barrier (20) with the circular base $a(\phi) = a_0$ the asymptotic formula (21) becomes exact for arbitrary q . This is confirmed by investigation presented in Table I which illustrates the convergence of the numerical values $f(q, \phi, \phi_q)$ with increasing ($U_0 \rightarrow \infty$) and narrowing ($a_0 \rightarrow 0$) of the potential barrier to the analytic result (21). In the limit case $U_0 \rightarrow \infty$ and $a_0 \rightarrow 0$ we obtain $a_{2D} \rightarrow a_0$ for the scattering length a_{2D} extracted from the calculated amplitude $f(q)$ by the formula (21), what is in agreement to the estimate given in [22]. The range of applicability of Eq. (21) was investigated recently in [28].

Then, we have applied our scheme for calculation of the scattering cross section $d\sigma(q, \phi, \phi_q)/d\Omega = |f(q, \phi, \phi_q)|^2$ for the isotropic ($a(\phi) = a_0$) and anisotropic ($a(\phi = \pi/2)/a(\phi = 0) = 1.1$ and 2) scattering. In Fig. 3 the differential cross section, calculated for the circular base $a(\phi) = a_0$ of the scatter (20), is given as a function of q and ϕ . The dependence of the cross

TABLE I. The dependence of the scattering amplitude $f(q, \phi, \phi_q)$ on the height of the potential barrier (20) with circular base. Calculations were carried out for $a_0 = 0.01$ with the parameters: $M = 10^2$, $N = 10^5$ and $\rho_N = 15$.

U_0	$q = 0.125$		$q = 1$	
	$f(q, 0, 0)$	$f(q, \pi, 0)$	$f(q, 0, 0)$	$f(q, \pi, 0)$
10^4	$-0.42692 + i0.08772$	$-0.42693 + i0.08772$	$-0.19832 + i0.05304$	$-0.19837 + i0.05304$
10^5	$-0.47960 + i0.11141$	$-0.47961 + i0.11141$	$-0.22999 + i0.07362$	$-0.23016 + i0.07362$
10^6	$-0.49055 + i0.11674$	$-0.49056 + i0.11674$	$-0.23673 + i0.07853$	$-0.23696 + i0.07853$
10^8	$-0.49400 + i0.11846$	$-0.49402 + i0.11846$	$-0.23895 + i0.07988$	$-0.23920 + i0.07988$
10^{10}	$-0.49408 + i0.11850$	$-0.49409 + i0.11849$	$-0.23899 + i0.07992$	$-0.23925 + i0.07992$
Eq.(21)	$-0.49486 + i0.11430$	$-0.49486 + i0.11430$	$-0.23901 + i0.07952$	$-0.23901 + i0.07952$

section on ϕ disappears with decreasing momentum q and the dependence on ϕ_q is absent for any q due to the spherical symmetry of the potential (20) if $a(\phi) = a_0$. Further, the analysis was extended to more general case of elliptical base of the potential barrier (20). In Figs. 4 and 5 the calculated differential cross sections on the anisotropic scatter (20) are presented for the cases of weak ($a(\phi = \pi/2)/a(\phi = 0) = 1.1$) and strong anisotropy ($a(\phi = \pi/2)/a(\phi = 0) = 2$). Here, we observe more sharp dependence on ϕ and q in the cross section with increasing anisotropy of the scatterer. The anisotropy in the scattering cross sections appears with increasing q earlier for the anisotropic potential barrier than for the barrier with circular base.

B. Dipole-dipole scattering in plane

Here we analyze the 2D quantum scattering on the long-range anisotropic scatterer defined by the dipole-dipole interaction. This problem simulates the collisions of polar molecules in pancake optical traps. The interaction potential between two arbitrarily oriented dipoles reads

$$U(\boldsymbol{\rho}, \mathbf{d}_1, \mathbf{d}_2) = \frac{1}{\rho^3} \left((\mathbf{d}_1 \mathbf{d}_2) - 3 \frac{(\mathbf{d}_1 \boldsymbol{\rho})(\mathbf{d}_2 \boldsymbol{\rho})}{\rho^2} \right), \quad (22)$$

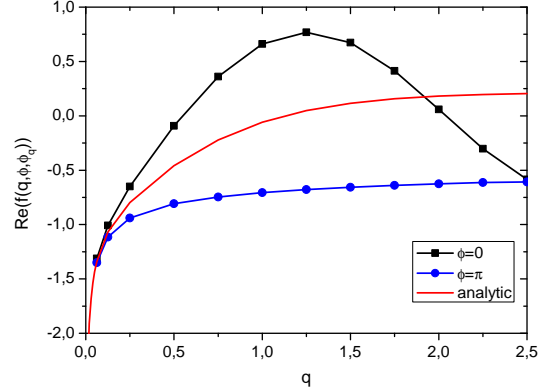
where \mathbf{d}_i , ($i = 1, 2$) – dipole moments and $(\mathbf{d}_i \boldsymbol{\rho})/\rho$ – their projections onto the collision axis. The expression (22) can be written in the polar coordinates

$$U(\rho, \phi; \alpha, \beta, \gamma) = \frac{d_1 d_2}{\rho^3} [\sin(\alpha) \sin(\gamma) \cos(\beta) + \cos(\alpha) \cos(\gamma) - 3 \sin(\alpha) \sin(\gamma) \cos(\phi) \cos(\phi - \beta)], \quad (23)$$

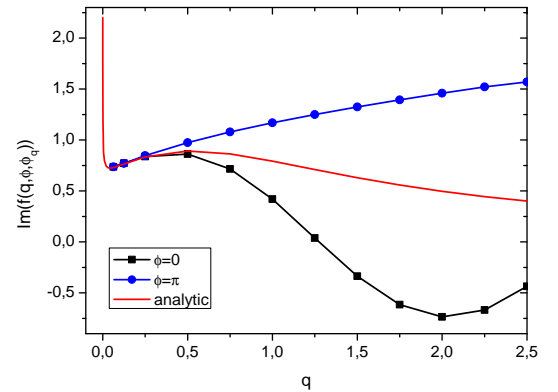
where the angles α and γ define the tilt of dipoles to the scattering plane XY and the angle β denotes the mutual orientation of the dipole polarization planes Zd_1 and Zd_2 in Fig. 6.

If we consider the scenario when the polarization of colliding molecules is orthogonal to the plane of motion ($\alpha = \beta = \gamma = 0$), interaction is fully isotropic and repulsive

$$U(\rho) = \frac{d_1 d_2}{\rho^3}. \quad (24)$$



a)



b)

FIG. 1. (Color online) The dependence of real a) and imaginary b) part of the scattering amplitude on the momentum q for the potential barrier (20) with circular base $a(\phi) = a_0 = 1$ and $U_0 = 10^4$. Calculations were carried out for $\phi_q = 0$ with the parameters: $M = 10^2$, $N = 10^5$ and $\rho_N = 15$.

This case was intensively studied in the previous works [16, 18].

For dipoles oriented in the plane ($\alpha = \gamma = \frac{\pi}{2}$), anisotropy

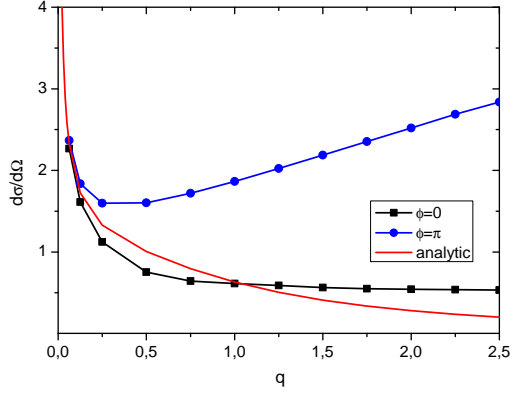


FIG. 2. (Color online) The dependence of the differential cross section on the momentum q for the potential barrier (20) with circular base $a(\phi) = a_0 = 1$ and $U_0 = 10^4$. Calculations were carried out for $\phi_q = 0$ with the parameters: $M = 10^2$, $N = 10^5$ and $\rho_N = 15$.

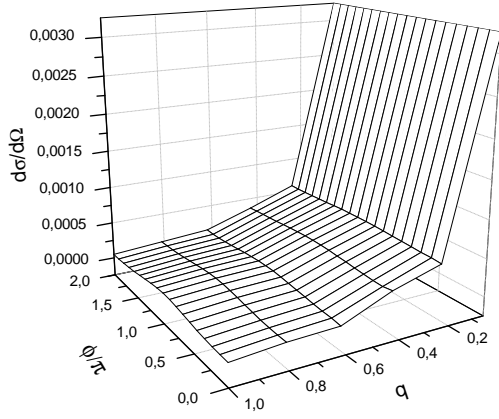


FIG. 3. The dependence of the differential cross section on the momentum q and scattering angle ϕ in the case of potential barrier (20) with $U_0 = 10^3$ and circular base $a(\phi) = a_0 = 1$. Calculations were carried out for $\phi_q = 0$ with the parameters: $M = 10^2$, $N = 10^5$ and $\rho_N = 15$.

arises and the interaction potential reads

$$U(\rho, \phi, \beta) = \frac{d_1 d_2}{\rho^3} [\cos(\beta) - 3 \cos(\phi) \cos(\phi - \beta)]. \quad (25)$$

A particular case of parallel dipoles with the polarization axis tilted to the plane of motion ($\alpha = \gamma$; $\beta = 0$) with short-range interaction modeled by a hard wall at the origin

$$V_{HW}(\rho) = \begin{cases} \infty, & \rho \leq \rho_{HW} \\ 0, & \rho > \rho_{HW} \end{cases} \quad (26)$$

with the width $\rho_{HW}/D = 0.1$

$$U(\rho, \phi, \alpha) = V_{HW}(\rho) + \frac{d^2}{\rho^3} [1 - 3 \sin^2(\alpha) \cos^2(\phi)] \quad (27)$$

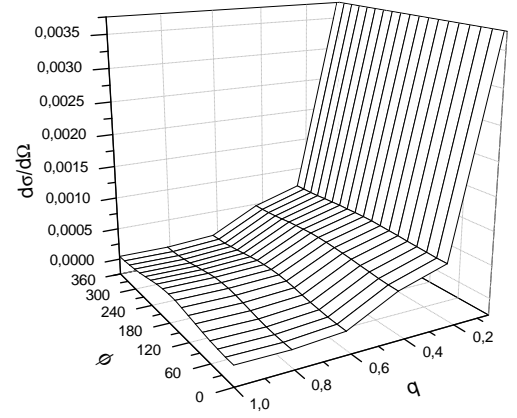


FIG. 4. The dependence of the differential cross section on the momentum q and scattering angle ϕ in the case of potential barrier (20) with $U_0 = 10^3$ and elliptic base with $a(\pi/2) = 1.1$ and $a(0) = 1$. Calculations were carried out for $\phi_q = 0$ with the parameters: $M = 10^2$, $N = 10^5$ and $\rho_N = 15$.

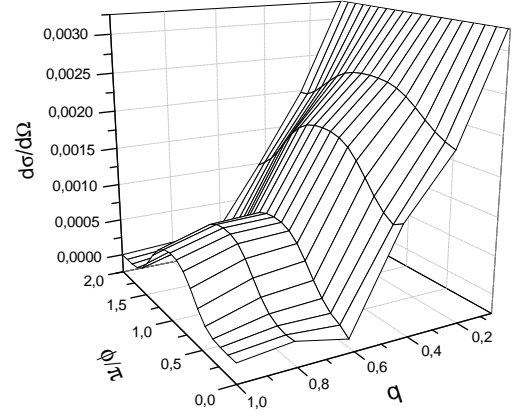


FIG. 5. The same as in Fig. 4 but for the case of strong anisotropy of the scatterer (20) with $a(\pi/2) = 2$ and $a(0) = 1$.

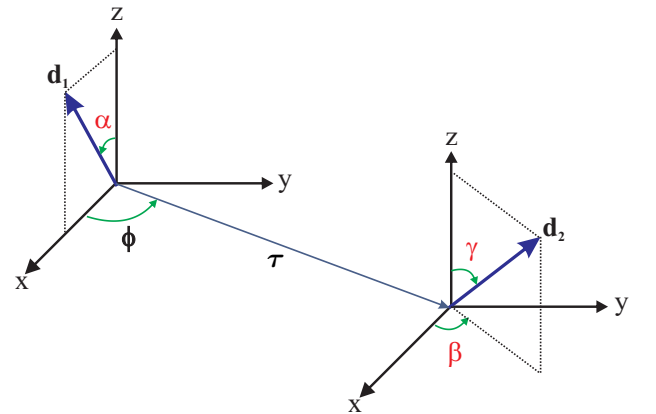


FIG. 6. (Color online) Collision in the plane XY of two arbitrarily oriented dipoles \mathbf{d}_1 and \mathbf{d}_2

was considered in paper [17]. We have investigated this case with our approach and have obtained good agreement with the results of paper [17]. This is illustrated by Fig. 7, where the calculated total cross section $\sigma(q, \alpha)$ (5) is given in the units of σ_{SC} . Here D is the dipolar length $D = \mu d^2 / \hbar^2$ ($d = d_1 = d_2$) and $\sigma_{SC} = \frac{4}{q} \sqrt{\pi D q}$ is the value of the total scattering cross section in the eikonal approximation that is valid in the high-energy regime, $Dq \gg 1$ [17]. All calculations in this section were performed for the following parameters: $M = 40$, $N = 1.2 \times 10^5$ and $\rho_N = 60$; the number of grid points on ϕ_q was $2M_q + 1 = 101$.

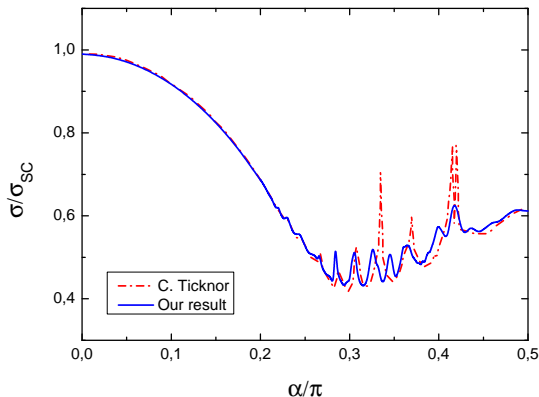


FIG. 7. (Color online) A comparison of the total cross section (in the units of σ_{SC}) with the result of C. Ticknor [17] calculated for potential (27) at $D = 1$, $Dq = 10$.

Then, we have analyzed how the found “resonant” structure for the polarized dipoles (see Fig. 7) in the calculated dependence of the scattering cross section on the dipole tilt angle $\alpha = \gamma$ varies with destroying the polarization. Depolarization was simulated by rotating the angle β between the dipole polarization planes Zd_1 and Zd_2 (see Fig. 6). We found progressive narrowing of the “resonance” area with a simultaneous decrease of the amplitudes of the “resonance” oscillations with increasing angle β from 0 to π (see Fig. 8). When approaching the point π the “resonant” structure disappears, the cross section becomes smooth relative to α and reaches its maximum value. This effect is due to the fact that when approaching the angle $\beta = \pi$ repulsive feature of the dipole-dipole interaction becomes dominant (see Fig. 9). With decreasing β from π to 0 the attractive part $U(\rho, \phi) < 0$ appears for some ρ and ϕ . It leads to appearing the “resonant” part in the scattering cross section. Note, that the presented cross sections were obtained for distinguishable particles. The effect of symmetrization/antisymmetrization $f_{g,u}(\phi) = (f(\phi) \pm f(\phi - \pi))/\sqrt{2}$ (i.e. transition to identical particles) is shown in Fig. 10 for $\alpha = 0.2\pi$ and β varying from 0 to 2π , where we observe the strong dependence of the total cross sections on the angle β with the maximal enhancement at $\beta = \pi$.

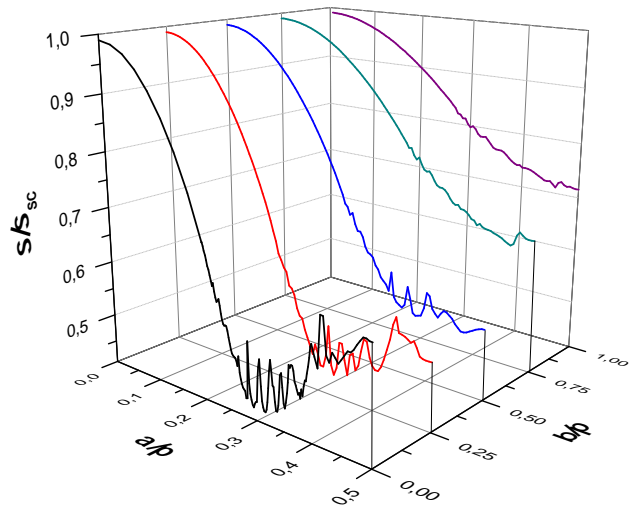


FIG. 8. (Color online) The total cross sections σ in the units of σ_{SC} as a function of the dipole tilt angle $\alpha = \gamma$ and the rotational angle β calculated for potential (23) at $D = 1$, $Dq = 10$.

The cross sections are symmetric with respect to this point. We have to note that the curves $\sigma_g(\beta)$ and $\sigma_u(\beta)$ describing the scattering of bosonic and fermionic particles exactly repeat the behavior of the curve $\sigma(\beta)$ for distinguishable particles.

Finally, we have analyzed the scattering of arbitrarily oriented dipoles in the case of mutual orthogonality of their polarization planes Zd_1 and Zd_2 ($\beta = \pi/2$). Here also we found a strong “resonant” structure by the tilt angle γ of one dipole, if the other dipole is oriented in the scattering plane XY ($\alpha = \beta = \pi/2$) (see Fig. 11), that appears due to the attractive feature of the dipole-dipole interaction strength with increasing of the tilt angle $\alpha \rightarrow \pi/2$.

IV. CONCLUSION

We have developed a computational scheme for quantitative analysis of the 2D quantum scattering on the long-range anisotropic potentials. High efficiency of the method was demonstrated in the analysis of scattering on the cylindrical potential with the elliptical base and dipole-dipole collisions in the plane. In the last case we found the strong dependence of the scattering cross section on the mutual orientation of dipoles.

The method can be applicable for analyzing the collisional dynamics of the polarized as well as unpolarized polar molecules in the plane. A natural application is the quantitative analysis of the confinement-induced resonances (CIR) in one-dimensional traps. Particularly, this analysis can resolve the puzzle with the position of

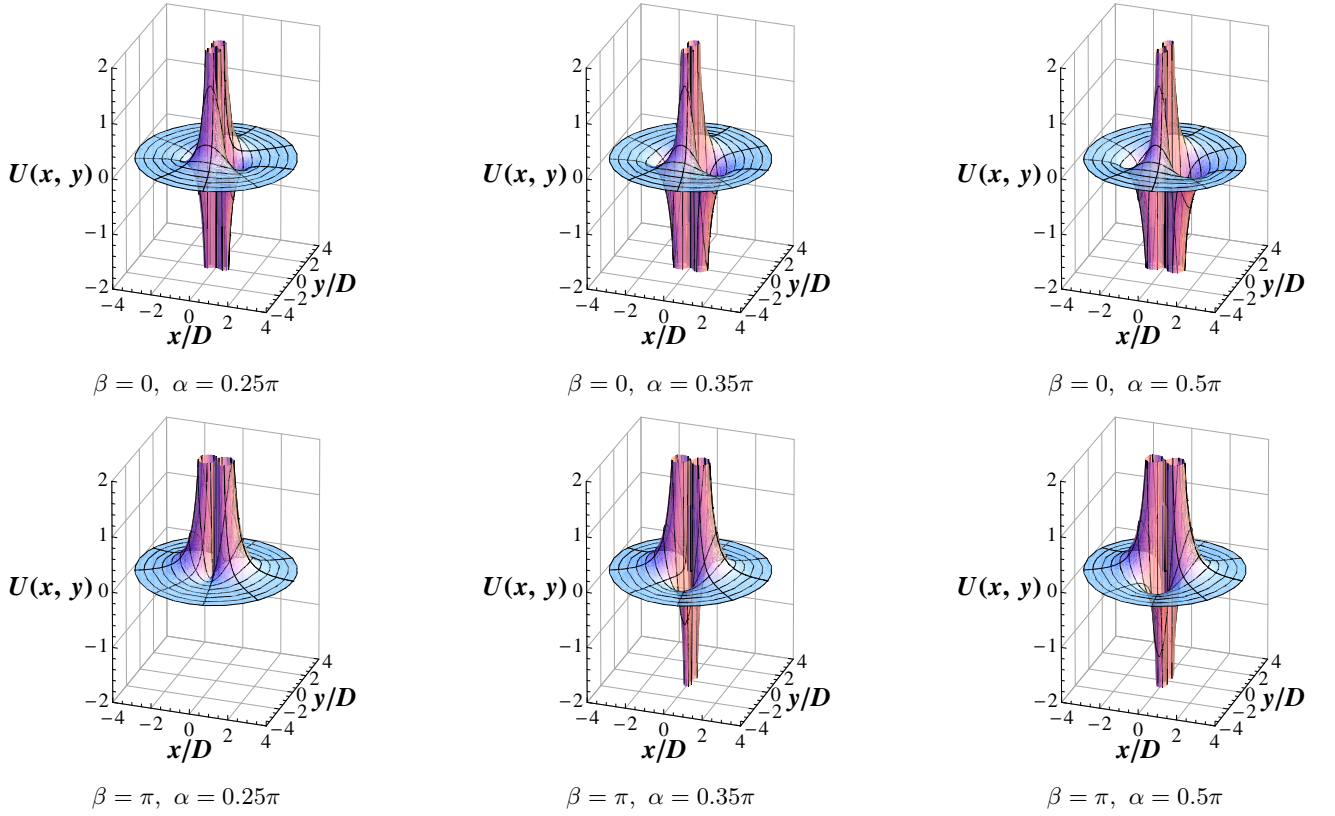


FIG. 9. (Color online) The dependence of the dipole-dipole potential $U(\boldsymbol{\rho}, \mathbf{d}_1, \mathbf{d}_2)$ (23) in the units of $E_D = \hbar^6 / \mu^3 d^4$ ($d = d_1 = d_2$) on the tilt angle α for two extreme mutual orientations $\beta = 0$ and π of the dipole polarization planes Zd_1 and Zd_2 .

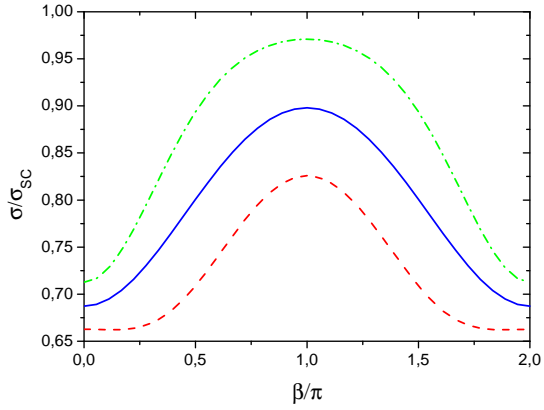


FIG. 10. (Color online) The total cross section σ (solid line), bosonic cross section σ_g (dashed line) and fermionic cross section σ_u (dash-dot line) calculated for potential (23) as a function of the angle β for the fixed $\alpha = 0.2\pi$ at $D = 1$, $Dq = 10$ (in the units of σ_{SC}).

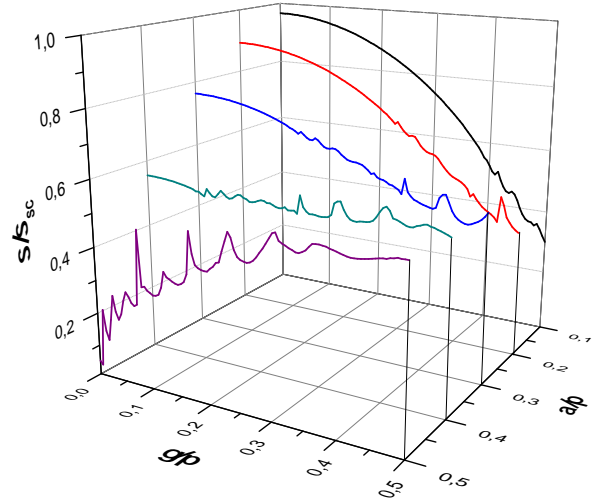


FIG. 11. (Color online) The total cross sections σ in the units of σ_{SC} as a function of the dipole tilt angles α and γ calculated for potential (23) at $D = 1$, $Dq = 10$. The rotational angle β is equal to $\pi/2$.

the 2D CIR measured recently [29], which is under intensive discussions.

TABLE II. The dependence of the scattering amplitude $f(q, \phi, \phi_q)$ on the number of angular grid points for the scatterer (20) with elliptical base. Calculations were performed for $q = 1.5$ with the parameters: $U_0 = 10^3$, $N = 10^4$, and $\rho_N = 15$.

M	$a_0(\pi/2)/a_0(0) = 1.1$		$a_0(\pi/2)/a_0(0) = 2.0$	
	$f(q, 0, 0)$	$f(q, \pi, 0)$	$f(q, 0, 0)$	$f(q, \pi, 0)$
1	0.94212 - i0.36446	-0.33027 + i1.24225	-0.95099 - i0.52976	0.36649 + i1.04884
2	0.65275 - i0.30331	-0.61946 + i1.30336	-1.48979 + i0.79336	-0.50755 + i2.02677
3	0.68693 - i0.30254	-0.65392 + i1.30275	-0.31229 + i0.79336	-1.01013 + i1.68129
4	0.68794 - i0.30507	-0.65902 + i1.29149	-0.28629 + i0.18596	-0.90989 + i1.50458
5	0.68799 - i0.30506	-0.65940 + i1.29164	-0.50155 + i0.05523	-0.87486 + i1.52425
10			-0.60611 + i0.07641	-0.89428 + i1.53586
20			-0.61098 + i0.07836	-0.89552 + i1.53816
30			-0.61173 + i0.07971	-0.89572 + i1.53885

-
- [1] M. A. Baranov, Phys. Rep. **464**, 71 (2008).
[2] I. Bloch, J. Dalibard and W. Zwerger, Rev. Mod. Phys. **80**, 885 (2008).
[3] C. Ticknor, R. M. Wilson and J. L. Bohn, Phys. Rev. Lett. **106**, 065301 (2011).
[4] G. M. Brunn and E. Taylor, Phys. Rev. Lett. **101**, 245301 (2008).
[5] J. C. Cremon, G. M. Brunn and S. M. Reimann, Phys. Rev. Lett. **105**, 255301 (2010).
[6] K.-K. Ni et. al., Science **322**, 231 (2008); S.Ospelkam et. al., Science **327**, 853 (2010).
[7] L. D. Carr et. al., New J. Phys **11**, 055049 (2009).
[8] M. H. G. de Miranda et. al., Nat. Phys. **7**, 502 (2011).
[9] P. Minnhagen, Rev. Mod. Phys. **59**, 1001 (1987).
[10] P. A. Lee, N. Nagaosa and X.-G. Wen, Rev. Mod. Phys. **78**, 17 (2006).
[11] K. S. Novoselov, Rev. Mod. Phys. **83**, 837 (2011).
[12] C. Nayak, S. H. Simon, A. Stern, M. Freedman and S. D. Sarma, Rev. Mod. Phys. **80**, 1083 (2008).
[13] K. Martiyanov, V. Makhalov and A. Turlapov, Phys. Rev. Lett. **105**, 030404 (2010); A. Turlapov, JETP Letters **95**, 96 (2012).
[14] M. Marinescu and L. You, Phys. Rev. Lett. **81**, 4596 (1998).
[15] V. S. Melezhik and Chi-Yu Hu, Phys. Rev. Lett. **90**, 083201 (2003).
[16] C. Ticknor, Phys. Rev. A **80**, 052702 (2009).
[17] C. Ticknor, Phys. Rev. A **84**, 032702 (2011).
[18] C. Ticknor, Phys. Rev. A **81**, 042708 (2010).
[19] J. P. D’Incao and C. H. Greene, Phys. Rev. A **83**, 030702 (2011).
[20] Z. Li, S. V. Alyabyshev and R. V. Krems, Phys. Rev. Lett. **100**, 073202 (2008).
[21] V. S. Melezhik, J. Comput. Phys. **92**, 67-81 (1991).
[22] L. D. Landau and E. M. Lifshitz, in *Quantum mechanics: Non-Relativistic Theory*, Vol. 3 (Pergamon Press, 1977) 3rd ed., Chap. 132, pp. 551–552.
[23] D. S. Petrov and G. V. Shlyapnikov, Phys. Rev. A **64**, 012706 (2001).
[24] L. D. Landau and E. M. Lifshitz, in *Quantum mechanics: Non-Relativistic Theory*, Vol. 3 (Pergamon Press, 1977) 3rd ed., Chap. 123, pp. 507–508.
[25] M. Abramowitz and A. I. Stegun, *Handbook of Mathematical Functions* (U.S. National Bureau of Standards, 1965).
[26] I. M. Gelfand and S. V. Fomin, *Calculus of Variations* (Dover Publications, New York, 2000).
[27] W. H. Press, S. A. Teukolsky, W. T. Vetterling, and B. P. Flannery, *Numerical Recipes* (Cambridge University Press, Cambridge, 1992).
[28] V. V. Pupyshev, JINR preprint P2-2012-119, Dubna (2012); Phys. Atom. Nucl. (in press)
[29] E. Haller et. al., Phys. Rev. Lett. **104**, 153203 (2010).